Unconventional, Amphiphilic Polymers Based on Chiral Poly(ethylene oxide) Derivatives. 2. Ordering and Assembly[1]

H. M. Janssen and E. W. Meijer*

Laboratory of Organic Chemistry, Eindhoven University of Technology, P.O. Box 513, 5600 MB, Eindhoven, The Netherlands

Received June 26, 1997; Revised Manuscript Received October 9, 1997[⊗]

ABSTRACT: The poly(ethylene oxide) derivatives **1**−**3** (Figure 1) are—in design—synthetic analogues of coiled-coil-forming peptides. A comparative optical rotatory dispersion (ORD) study and TEM measurements have been used to investigate the ordering and assembly processes that are involved in the aggregation of these amphiphilic polymers **1**−**3** in H_2O. ORD measurements have shown that various ethylene oxide derivatives display an inversion of optical rotation upon complexation with KSCN, i.e. upon adoption of a helical conformation. This observation has led to the proposal that polymers **1**−**3** are helically ordered in H_2O, since the methyl-substituted polymer **3** exhibits an inversion of optical rotation on going from apolar (THF) to polar (H_2O) solvents; phase separation prohibits the detection of such an inversion for the isobutyl-substituted polymers **1** and **2**. TEM studies on surfaces onto which polymers **1**−**3** were deposited from aqueous solutions revealed granular and threadlike aggregates. The formation of the threadlike higher structures requires a *directionality* in the assembly process. Such a directionality could be provided by the formation of coiled-coil tertiary structures. However, *substantial* evidence for the formation of coiled coils or other specific tertiary structures is lacking.

Introduction

Nature provides us with an almost infinite number of well-defined, functioning, supramolecular systems[2] and therefore gives inspiration to chemists in their search for useful, new architectures. The construction of synthetic equivalents of structures found in nature is challenging and may eventually lead to new insights in the development of materials with unique and previously unattainable properties. The ongoing activity in the field of supramolecular chemistry has, for instance, led to the synthesis of an equivalent of the tobacco mosaic virus, in the sense that the spatial design of the virus has been copied in a synthetic system.[3] An elegant supramolecular structure found in certain peptides is the so-called coiled coil:[4] a structure of associated α-helices, which was modeled for the first time theoretically by Crick in 1952[5] and for which the first precise X-ray data were published almost 40 years later by O'Shea.[6] In recent years, coiled-coil superstructures have received enormous attention.[7] Not only naturally occurring proteins[8] but also synthetically designed polypeptides[9] have been investigated in order to distinguish between the different factors that are involved in the formation of coiled coils. It is now generally accepted that coiled coils are formed due to hydrophobic interactions between the α-helical parts; these parts have a 3,4 repeat (also called a 7_2-repeat) of apolar amino acids in a polar sequence of amino acids. As a result, the hydrophobic residues are directed in an apolar ribbon along the surface of the α-helix. At the right pH, the 'ribbon-type' of amphiphiles associate in H_2O to bundles of superhelices.

The formation of well-defined, secondary or tertiary structures is not confined to (natural) peptides, since numerous synthetic polymers can form ordered structures, especially in the solid state (e.g. helical arrangements are quite common secondary structures for synthetic polymers;[10] a few synthetic polymers form so-called stereocomplexes[11,12]). However, to our knowledge, coiled-coil formation of synthetic polymers involving hydrophobic interactions has never been reported.[13]

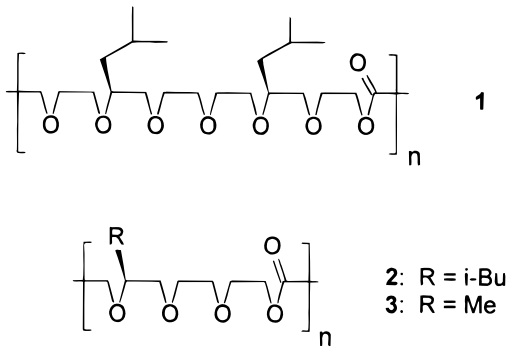

Figure 1. PEO-based polymers **1**−**3**: analogues—in primary structure—of coiled-coil-forming peptides.

The PEO-based synthetic polymers **1-3** shown in Figure 1 are designed to form coiled-coil superstructures on the basis of hydrophobic interactions. Their primary structure is a repeat of polar ethylene oxide units and apolar, alkyl-substituted ethylene oxide units, addressing the repeat of polar and apolar units in coiled-coil-forming peptides. The isobutyl and methyl side-chains in **1**−**3** are placed not only in a regioregular fashion but also in a stereoregular fashion, mimicking the chirality in peptides. Additionally, PEO forms 7_2 helices in the solid state,[14] and PEO has a tendency to form helical arrangements in dilute aqueous solutions.[15] Therefore, it is possible that the PEO-based polymers **1**−**3** form 'ribbon-type' amphiphiles—i.e. helices that have an apolar and a polar face—and it can further be imagined that these amphiphiles associate to coiled-coil superstructures in H_2O.

It has been shown in the preceding paper that the poly(ethylene oxide(derivatives **1**−**3** form aggregates in aqueous solutions at 20 °C as a result of their amphiphilic behavior. In this paper, it is investigated whether this aggregation is accompanied by the formation of well-defined structures such as coiled coils. In a more general sense, the ordering and assembly of **1**−**3** is investigated here. The chirality in macromolecules

[⊗] Abstract published in *Advance ACS Abstracts,* December 15, 1997.

S0024-9297(97)00939-X CCC: $14.00

1−**3** is used to perform a *comparative* study, using optical rotatory dispersion (ORD) spectroscopy. ORD spectra of polymers **1**−**3** in various solvents and under various conditions are related to each other and to ORD spectra of similar, oligomeric or polymeric reference components. The synthesis and characterization of these oligomeric and polymeric species are also described here. Additionally, polymers **1**−**3** are studied by microscopy techniques—mainly transmission electron microscopy (TEM)—to examine the aggregates that are formed in H_2O.

Results and Discussion

Approach. Coiled-coil superstructures can conveniently and in detail be examined by investigation of the X-ray data of crystals of coiled-coil-forming peptides.[6] In solution, CD spectroscopy of α-helical peptides is a simple and powerful technique to determine the formation of coiled-coil structures.[16] In contrast to peptides, polymers **1**−**3** are not monodisperse, so the crystallization of these sticky oils would be even more laborious than that for peptides and is presumably not possible at all. Also, the extensive knowledge on the chiroptical behavior of α-helical peptides cannot be used in a study of aqueous solutions of polymers **1**−**3** (because these polymers are constituted differently). The possibility of the formation of well-defined structures by polymers **1**−**3** in aqueous solutions can therefore be studied by (i) developing new characterization methods, (ii) screening existing characterization methods and testing whether these methods can be applied to the characterization of the systems under investigation, and (iii) using various microscopy methods to directly observe the structures or aggregates that are formed. Since option (i) is not connected to our field of research, this option was not investigated. Option (ii) has extensively been examined here—ORD spectroscopy has been screened—and results on (iii) are also reported in this work.

Optical activity is strongly dependent on conformational equilibria,[17] and, therefore, circular dichroism (CD) and optical rotatory dispersion (ORD) spectroscopy are two techniques that can give telling information on the spatial arrangement of molecules *in solution*. ORD spectroscopy has been used in various studies on the conformational behavior of macromolecules. Coil−helix transitions in poly(amino acids) in general,[18] and in poly(γ-benzyl-L-glutamate), poly(β-benzyl-L-aspartate), and poly(λ-glutamic acid) in particular,[19] can be monitored by measuring the specific optical rotation at the Na D line. In several studies by Pino[20] and others,[21] synthetic polymers—including PPOs (poly(propylene oxides))—have been studied by ORD spectroscopy.

Synthesis of the Molecular Components. All oligomeric and polymeric species that have been used as reference components for polymers **1**−**3** are shown in Figure 2. The syntheses of polymers **1**−**3** and of compounds *(SS)*-**4** and *(SS)*-**8** have been reported in Part 1. *O*-Monobenzyl hexaethylene glycol has been described elsewhere.[22]

Oligomer **5** was synthesized by protection of *O*-monobenzyl hexaethylene glycol with MEMCl in refluxing CH_2Cl_2, employing $N(i\text{-}Pr)_2Et$ as HCl scavenger. Production of the quinoline-derivatized oligomer *(SS)*-**6** was achieved by tosylation of the α,ω-diol *(SS)*-**8** in CH_2Cl_2 using KOH as base and by coupling of the resulting tosylate *(SS)*-**9** with 8−hydroxyquinoline (Scheme 1). Yields exceeding 85% could be obtained for both steps.

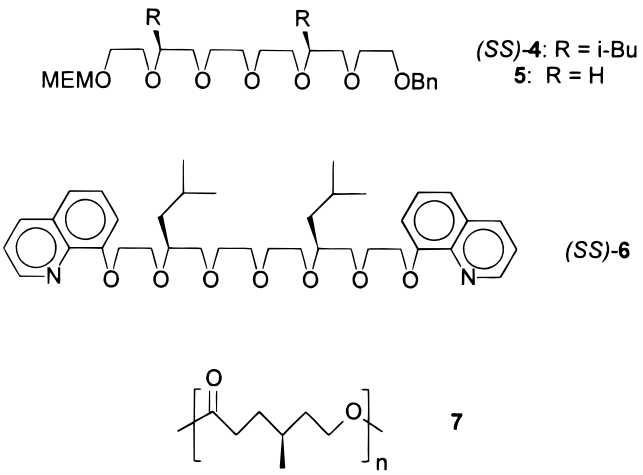

Figure 2. Synthesized reference components for polymers **1**−**3**.

Scheme 1. Synthesis of Oligomer *(SS)*-6[a]

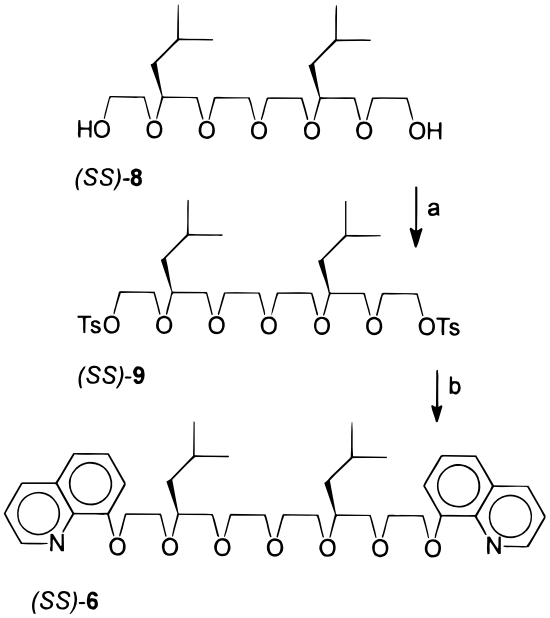

[a]Key: (a) TsCl, KOH, CH_2Cl_2, 0 °C (87%); (b) 8-hydroxyquinoline, KOH, HMPA, THF, Δ (85%).

Scheme 2. Polymerization of 4*(S)*-Methyl-ϵ-caprolactone Using $SnOct_2$ as Catalyst

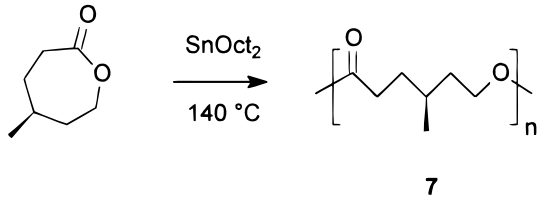

Poly(4*(S)*-methyl-ϵ-caprolactone) (**7**) was prepared as reference polymer for polymer **3** (Scheme 2). The enantiomerically pure 4*(S)*-methyl-ϵ-caprolactone was obtained in an enzymatically controlled Baeyer−Villiger oxidation of 4-methylcyclohexanone.[23] Polymerization of the *(S)*-monomer was performed at 140 °C using stannous 2-ethylhexanoate ($SnOct_2$) as catalyst. Two monomer/catalyst molar ratios were applied: a ratio of 98/1 gave a sticky oil with a molecular weight (M_n) of 8.4 kg/mol and a dispersity of 2.3, whereas a ratio of 810/1 gave polymeric material with an increased molecular weight of M_n = 29.7 kg/mol and a decreased

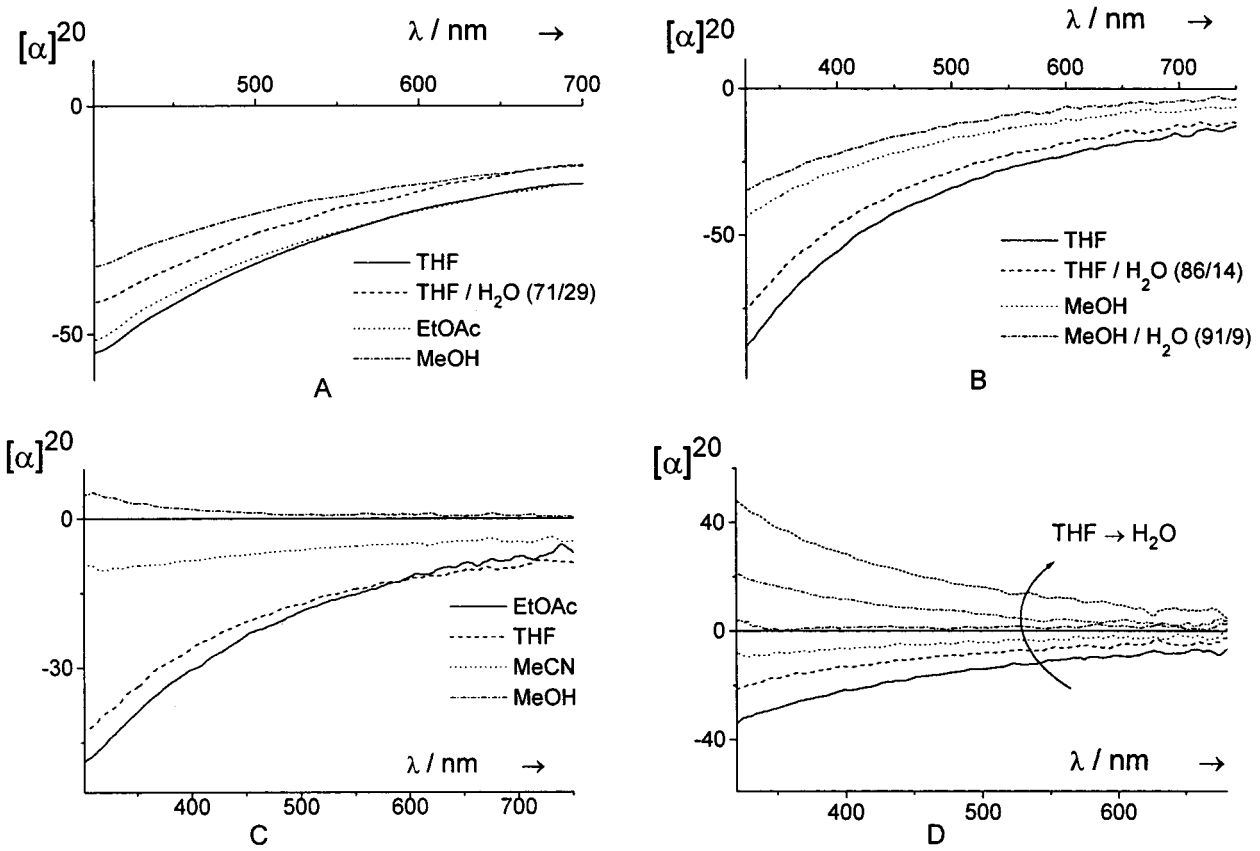

Figure 3. ORD spectra of polymers **1** (plot A), **2** (plot B), and **3** (plots C and D) in various solvents at 20 °C. Specific rotations [α] at 20 °C are plotted against the wavelength λ. Concentrations of ca. 2.5, 10, 15, and 1.5 mg/mL have been applied for plots A, B, C, and D, respectively. Solvent−solvent compositions are denoted in *v*/*v* ratios. In plot D, volume ratios of H_2O of 0%, 6%, 17%, 31%, 55%, and 100% have been used (see Experimental Section for details).

dispersity of 1.4. The latter polymer was also a sticky oil.

Ordering Processes of Polymers 1−3 in Aqueous Solutions: An ORD Analysis. Polyethylene oxide derivatives **1**−**3** were studied by ORD spectroscopy in various solvents ranging from apolar EtOAc to polar aqueous solvents. The behavior of the polymers in aqueous solutions had our special interest, since in these solutions hydrophobic interactions can play a role. Reliable ORD spectra can only be recorded when the solutions under investigation are sufficiently concentrated, homogeneous, transparent, and not macroscopically ordered (not birefringent). In practice, ORD spectroscopy of materials without chromophores or large dipoles is performed at concentrations ranging from approximately 0.1 mg/mL to 30 mg/mL. However, in this concentration range, polymeric solutions of **1**, **2**, and **3**, in pure H_2O are stable turbid solutions or give macroscopic phase separation (solutions of **1**, **2**, and **3** in H_2O become transparent at concentrations lower than ca. 0.1, 0.3, and 1.0 mg/mL, respectively[24]).

The aggregation of polymer **3** in H_2O at 20 °C was monitored by ORD spectroscopy. The methyl-substituted polymer **3** is the only polymer for which such a monitoring experiment is possible, since the critical association concentration (cac) of **3** is sufficiently high to allow ORD experiments (the cac of **3** is ca. 0.15 mg/mL[24]). ORD spectra of **3** were recorded at concentrations as low as 0.12 mg/mL (at which the polymer is molecularly dissolved) to concentrations as high as 1.4 mg/mL (at which the aqueous solution is hardly turbid and at which the polymer is aggregated). No change in specific rotation was observed upon the increase of the polymer concentration; invariably a positive specific rotation of the same magnitude was found. It can therefore be concluded that association of polymer **3** does not have any effect on the measured optical rotation.

The next step in the ORD analysis of polymers **1**−**3** involved the chiroptical behavior of **1**−**3** in solvents of varying polarity. In contrast to the positive specific rotation of **3** in H_2O, all polymers displayed a negative specific rotation in THF. In Figure 3, the results of the ORD measurements at 20 °C are depicted. All polymers showed the same trend: increasing the polarity of the solvent induced a less negative specific rotation. In particular for polymer **1**, but also for polymer **2**, no dramatic changes in specific rotation could be induced by changing the polarity of the solvent (plots A and B in figure 3), whereas—in contrast—polymer **3** displayed an inversion in optical rotation going from apolar to polar solvents, i.e. going from EtOAc or THF to MeOH or H_2O (see plots C and D). This inversion is *only* caused by the change in polarity of the solvent and *not* by the aggregation of the polymer, as evidenced by the ORD data reported in the previous paragraph. To put these initial ORD spectroscopy results in perspective, several reference ORD spectra have been recorded.

Oligomer *(SS)*-**4** and poly(*4(S)*-methyl-ϵ-caprolactone) (**7**) were selected as reference materials for polymers **1** and **2** and polymer **3**, respectively. The oligomer and the polymer were dissolved in MeOH and dioxane, respectively. While H_2O was added to both solutions, the specific rotation at 20 °C was monitored by recording ORD spectra. For both reference experiments, less negative rotations were observed upon increasing sol-

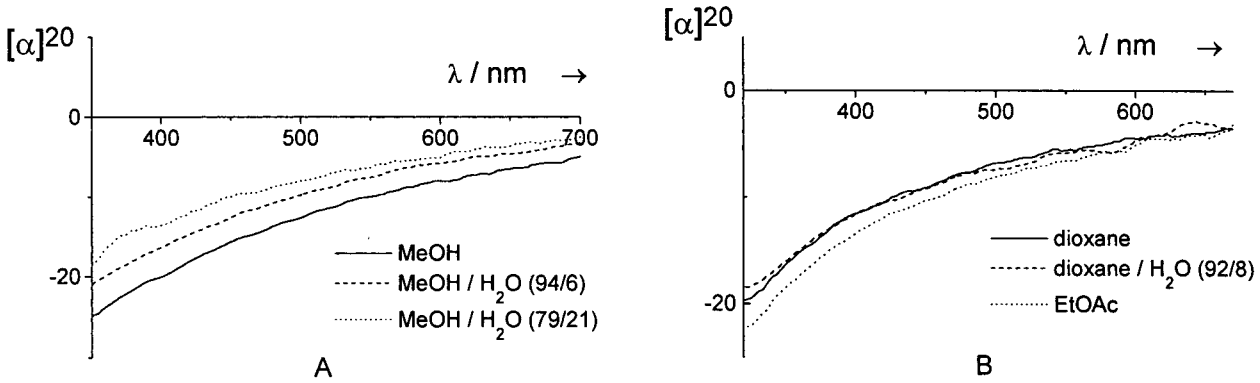

Figure 4. ORD spectra of oligomer *(SS)*-**4** (plot A) and poly(4*(S)*-methyl-ϵ-caprolactone) (**7**) (plot B) in various solvents at 20 °C. Specific rotations $[\alpha]^{20}$ are plotted versus the wavelength λ. Concentrations of approximately 4 and 3 mg/mL have been used in plots A and B, respectively. Solvent−solvent ratios are denoted in *v*/*v* ratios. See Experimental Section for details.

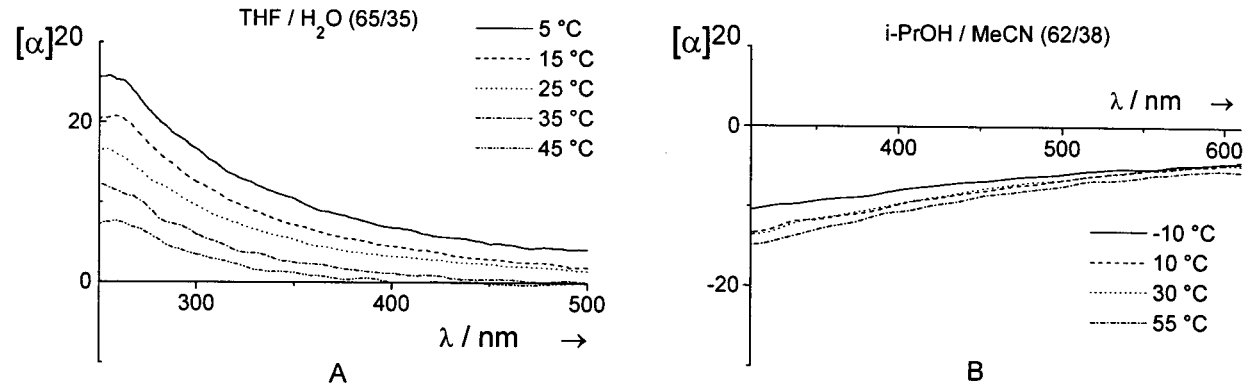

Figure 5. ORD spectra of polymer **3** in THF/H_2O (65/35) and in i-PrOH/MeCN (62/38) at different temperatures. Specific rotations [α] are plotted versus the wavelength λ. Concentrations of 24.4 and 17.9 mg/mL are used in plots A and B, respectively. Solvent−solvent compositions are denoted in *v*/*v* ratios. See the Experimental for details.

vent polarity, but no spectacular changes in specific rotation could be induced (see Figure 4; plots A and B). The combined experimental data of Figures 3 and 4 show that the chiroptical behavior of the methyl-substituted polymer **3** is anomalous: it is the only investigated material that shows an inversion in optical rotation upon increasing the polarity of the solvent. In the literature, such inversions of chiroptical rotation have seldom been described for polymers and have usually been related to ordering processes of the polymers involved.[25]

We propose that the inversion in optical rotation of polymer **3** upon increasing the polarity of the solvent signifies a distinct conformational transition in this polymer. Presumably, polymer **3** has a random conformation in good solvents such as EtOAc and THF and is more ordered conformationally in polar solvents such as MeOH and particularly H_2O. Possibly, also polymers **1** and **2** are more ordered conformationally in pure H_2O. However, an inversion in optical rotation upon increasing water content cannot be measured for aqueous solutions of **1** and **2**, since these polymers are not sufficiently soluble in H_2O.

Finally, ORD spectra of polymer **3** at various temperatures have been recorded. From Figure 5A, it is apparent that the specific rotation of an aqueous solution of polymer **3** becomes less positive with temperature. Thus, an increase in temperature of an aqueous solution of **3** has a similar effect on the monitored specific rotation as a decrease in polarity of the solvent would have. In Figure 5B, it is shown that a temperature increase in more apolar solvents hardly changes the specific rotation of polymer **3**. These results are in line with the previously mentioned hypothesis or proposal. A higher temperature enlarges the rotational freedom of polymer **3** in aqueous solution and will result in a less ordered conformation of this macromolecule (figure 5A). When the conformation of the polymer is already less ordered, as proposed for polymer **3** in apolar i-PrOH/MeCN solutions, an increase in temperature can hardly result in a dramatic change in conformation (Figure 5B).

In the described ORD analysis, it has been argued that the conformation of polymers **1**−**3** is more ordered in polar solvents than in apolar solvents. Reference data of known and extensively studied ordering processes of ethylene oxide compounds can lead to a more defined hypothesis concerning the *nature* of the proposed conformational order in the ethylene oxide derivatives in polar solvents. The complexation of ethylene oxide compounds with alkali salts is such an extensively studied ordering process.

Complexation of Chiral Ethylene Oxide Derivatives with Alkali Salts. Crystal structures of a wide variety of complexes of ethylene oxide compounds with salts have been reported, including crown ether complexes and complexes of linear, oligomeric ethylene oxides with alkali salts.[26] Especially the linear, oligomeric ethylene oxides are of relevance to this work, because these glycol derivatives are most related to the systems we are interested in. Vögtle and co-workers[26] have shown that larger oligomeric species fold into helical conformations in complexes with alkali salts. As an example, the crystal structure of RbI with α,ω-*O*,*O*′-diquinolinyl-modified tetraethylene glycol is shown in Figure 6.

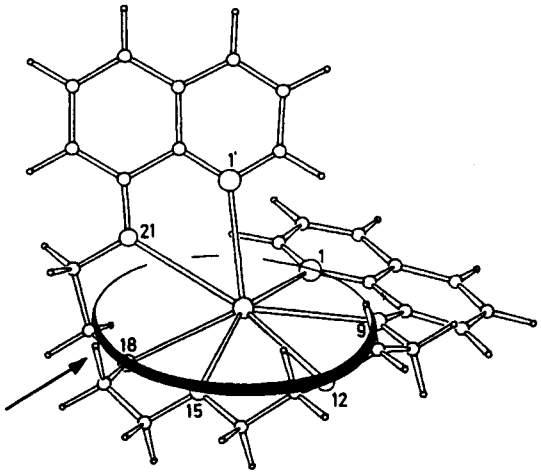

Figure 6. Crystal structure of the α,ω-O,O′-diquinolinyl tetraethylene glycol−RbI complex. The dihedral angle causing the helical structure of the molecule is indicated with an arrow.[29]

In analogy to the work of Vögtle, the complexation of the ethylene oxide oligomers *(SS)*-**4**, **5**, and *(SS)*-**6** (all three pictured in Figure 2) with the alkali salts RbI, NH_4PF_6, and—in most cases—KSCN was studied. Initially, cocrystallization of the oligomers with KSCN was attempted. Standard procedures for the synthesis of cocrystals of KSCN with either the diisobutyl-substituted *(SS)*-**4** or the unsubstituted oligomer **5** failed. Vögtle has shown that the introduction of quinoline end groups increases the impetus of ethylene oxide derivatives toward cocrystallization with alkali salts.[26] Therefore, it was attempted to obtain cocrystals of compound *(SS)*-**6** with KSCN or RbI. Again, all standard procedures failed. Apparently, the introduction of asymmetrical features in ethylene oxide compounds—alkyl side-chains—blocks the ability of these compounds to form cocrystals with alkali salts. Consequently, solid state data of the desired complexes could not be obtained and the study of these complexes was confined to the solution state.

^{1}H NMR, ^{13}C NMR, and ORD spectroscopy have been used to examine the complexation of the ethylene oxide oligomers *(SS)*-**4**, **5**, and *(SS)*-**6** with alkali salts in MeOH (again, KSCN was typically used). The titration of *(SS)*-**4** with KSCN in CD_3OD at 20 °C was monitored by ^{13}C NMR, and all carbon signals of *(SS)*-**4** shifted upon addition of KSCN (Figure 7A). A Job plot was constructed to investigate the stoichiometry of the complex, and it was established that in CD_3OD a 1:1 complex is formed (Figure 7B). The induced shifts of the carbon signals were plotted against the KSCN-concentration, and fitting of the data gave an association constant (*K*) for the *(SS)*-**4**−KSCN complex of approximately 35 L/mol (Figure 7C). When the complexation at 25 °C was monitored by measuring the specific rotation at the Na D line ($\lambda = 589$ nm), a *K* value in the same range was found ($K = 29$ L/mol, Figure 7D).

The complexation of the quinolinyl-functionalized ethylene oxide *(SS)*-**6** with KSCN was also studied. An association constant of 330 L/mol for the 1:1 complex was determined in CD_3OD at 20 °C by monitoring the ^{13}C NMR spectra upon titration with KSCN. Thus, the effect observed by Vögtle[26] is confirmed: the introduction of quinoline end groups increases the stability of glycol−KSCN complexes. Compared to that of the *(SS)*-**4**−KSCN complex, the Gibbs free energy for complexation is ca. 5.5 kJ/mol lower for the *(SS)*-**6**−KSCN complex. The association constant of the complex of unsubstituted oligomer **5** with KSCN in CD_3OD at 20 °C was also determined employing ^{13}C NMR and was found to be 25 L/mol. This value for the 1:1 complex is in the same order of magnitude as the *K* value of the *(SS)*-**4**−KSCN complex. Apparently, the introduction of isobutyl side chains to linear ethylene glycol compounds does not dramatically influence the stability of the complexes these compounds can form with alkali salts in solution.

The complex formation of oligomers *(SS)*-**4** and *(SS)*-**6** with KSCN in MeOH at 20 °C was monitored by ORD spectroscopy. The results of the titrations of *(SS)*-**4** and *(SS)*-**6** with KSCN are shown in Figure 8A and B, respectively. Similar results were obtained for both oligomers: complexation gave an inversion of specific optical rotation $[\alpha]_\lambda^{20}$. Analogous to the complexation of oligomeric species *(SS)*-**4** and *(SS)*-**6** with KSCN in MeOH, the complexation of polymers **1**−**3** with KSCN in MeOH was also monitored by ORD-spectroscopy. Polymers **1** and **2** displayed inversions of optical rotation, whereas polymer **3** gave an increasing specific optical rotation as complexation proceeded (polymer **3** without added KSCN already has a positive specific rotation in MeOH, see Figure 3C). We interpret these inversions as conformational changes from an approximately random conformation to a helical conformation, assuming a similar geometry of the ethylene oxides in solution and in the solid state (see Figure 6 for a helical conformation of a complexed ethylene oxide in the solid state).

When all ORD data (Figures 3−5 and 8) are combined, it can be imagined that in the studied ethylene oxide systems—i.e. polymers **1**−**3** and their oligomeric reference compounds—an inversion of optical rotation stems from a conformational transition from an approximately random arrangement to a more helically ordered arrangement. It is therefore proposed that polymer **3** and possibly polymers **1** and **2** are helically ordered in H_2O (the ORD data do not give definite *proof*, but *all* ORD data are in accordance with this for this proposition).

The described ORD measurements can give information on the conformational behavior of polymers **1**−**3** in aqueous solutions. However, a solid rationale concerning the probability of the formation of well-defined tertiary structures by these polymers in aqueous solutions cannot be inferred from the ORD-data available. The assembly of polymers **1**−**3** in H_2O can be studied in more detail applying various microscopy techniques. With these techniques the shapes of the formed aggregates can be examined.

Microscopy Studies on Polymers 1−3. Nanoscopic and microscopic structures formed by materials in solution can be studied by various microscopy techniques, such as atomic force microscopy (AFM)[27], scanning tunneling microscopy (STM),[27] and transmission electron microscopy (TEM). The only assumption that usually has to be made is that the observed structures on the substrate surfaces are representative for the structures that are formed in aqueous solutions.

TEM has been chosen to study the aggregation behavior of **1**−**3** in detail. Solutions of polymers **1**−**3** in H_2O, ranging from the dilute transparent solutions to the concentrated turbid solutions, were investigated. A range of sample preparation techniques was used, either carbon or polymer (formvar) surfaces were applied, and both uranyl acetate negative staining and Pt-

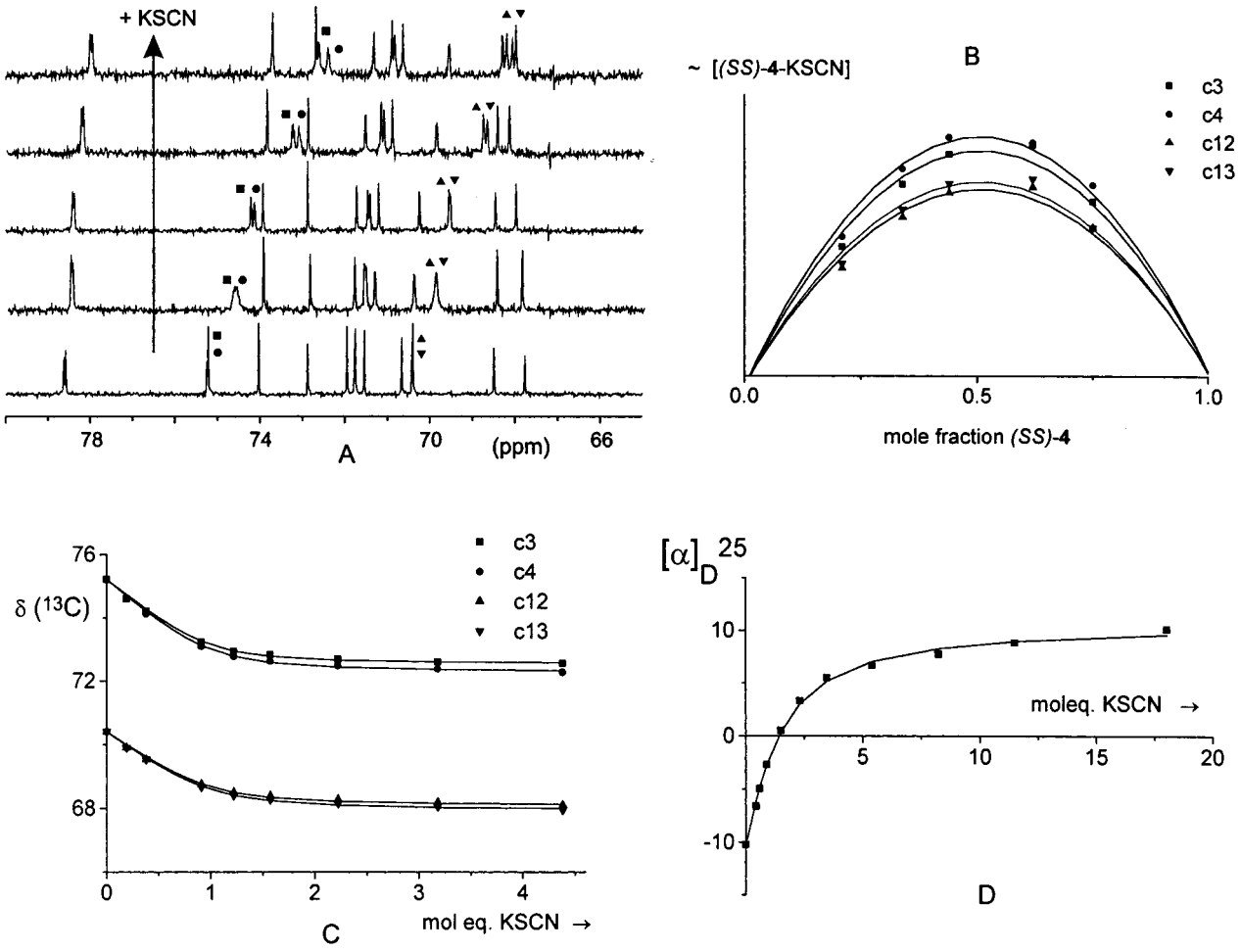

Figure 7. Complexation of compound *(SS)*-**4** with KSCN in CD_3OD or MeOH: (A, B, and C) complexation at 20 °C monitored by ^{13}C NMR spectroscopy; (A) indicated carbons c3, c4, c12, and c13 (■, ●, ▲, and ▼, respectively) shifting upfield upon complexation; (B) Job plot of complex formation, constructed with the data on carbons c3, c4, c12, and c13 (An arbitrary unit that scales with the concentration of the complex is plotted against the mole fraction of *(SS)*-**4**); (C) δ-Values of carbons c3, c4, c12, and c13 plotted against the molar equivalents of KSCN added (The solid lines indicate the best fits of the data); (D) complexation at 25 °C monitored by the specific optical rotation at the Na D line (The best fit of the data is indicated with the solid line). See the Experimental Section for details.

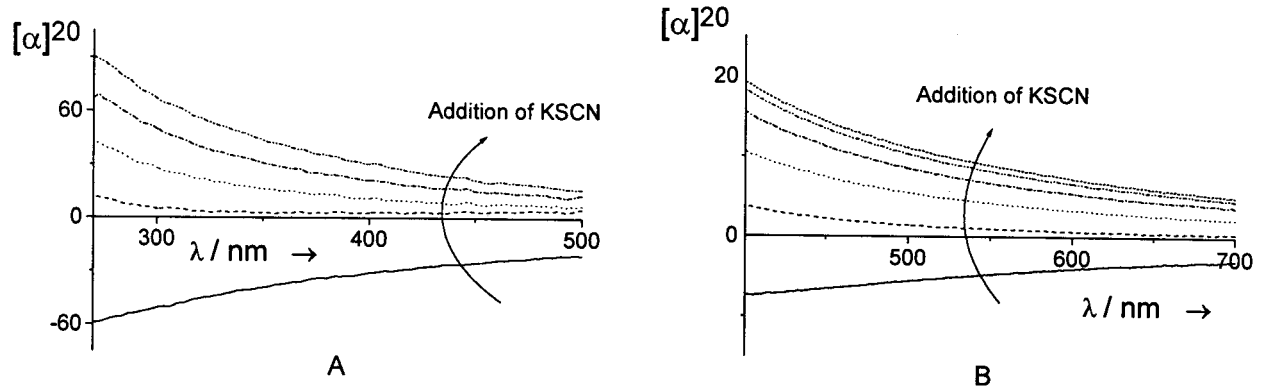

Figure 8. Complexation of *(SS)*-**4** (plot A) and *(SS)*-**6** (plot B) with KSCN in MeOH at 20 °C monitored by ORD spectroscopy. An inversion of specific optical rotation is observed upon titration with KSCN. The specific rotation $[\alpha]^{20}$ is plotted against the wavelength λ in nanometers. Concentrations of 0.0145 and 0.020 mol/L have been used for *(SS)*-**4** and *(SS)*-**6**, respectively. See the Experimental Section for details.

shading were employed to make detection of the formed structures possible. TEM pictures have been collected in Figure 9 to illustrate the observed structural features. On most grids, clusters of granular structures and clusters of threadlike structures were found (the threadlike structures were not found for the methyl-substituted polymer **3**). The dimensions of the granules and the 'threads' were in the range 10−50 nm (see the Experimental Section for details). In addition to the granules and 'threads', vesicle-like structures were observed. However, these vesicle-like structures were only found on one grid.

In conclusion, macromolecules **1**−**3** aggregate in H_2O to diversely shaped higher structures; structures such as those generally observed for amphiphiles. Most strikingly, threadlike structures have been found for

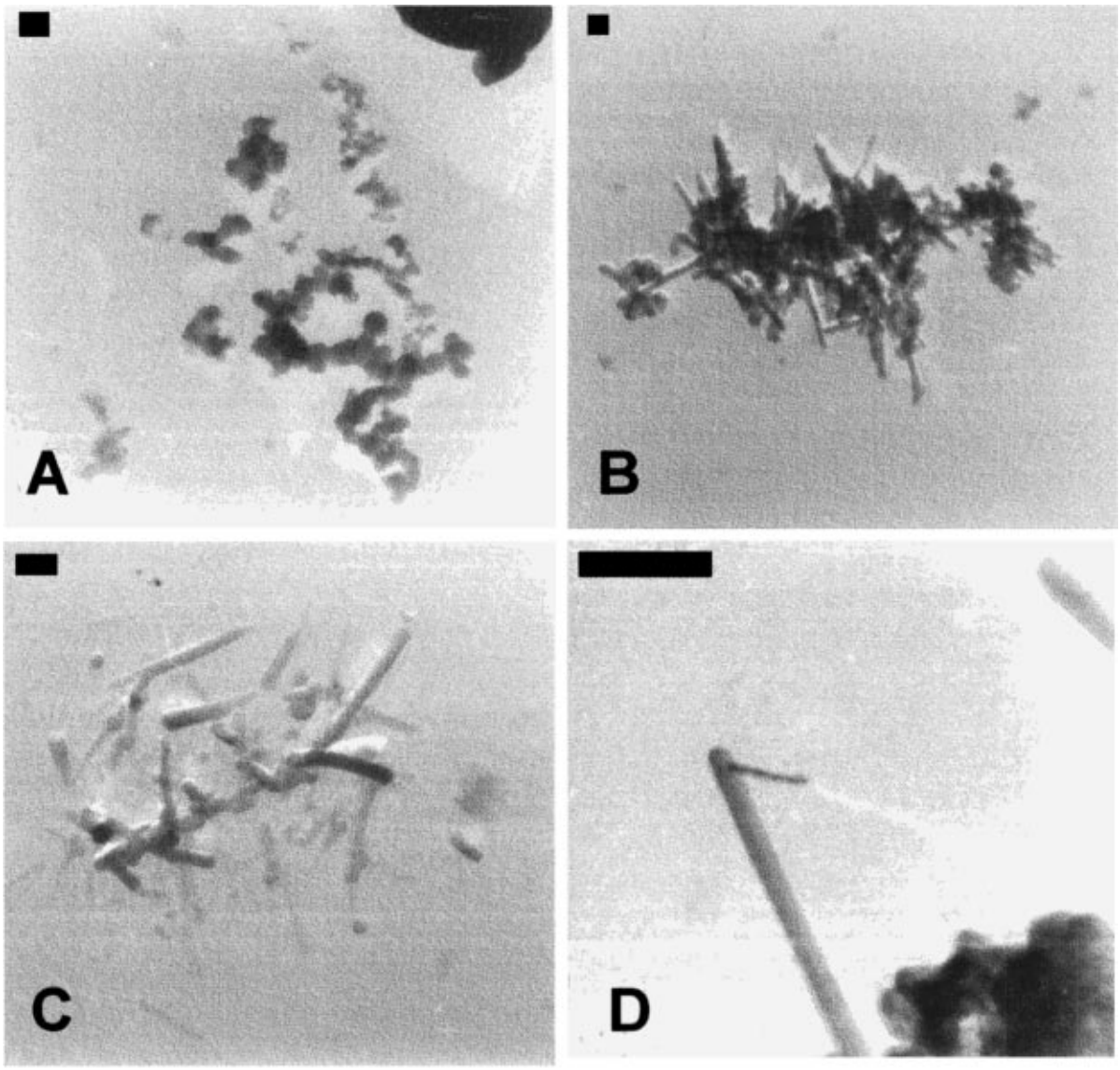

Figure 9. TEM pictures illustrating the aggregates formed by **1**, **2**, and **3**. Granular structures (for **1**, **2**, and **3**) and threadlike structures (for **1** and **2**) have been observed. The granules were ca. 50 nm in diameter, and the threads were 8−50 nm in diameter and 80−400 nm in length. (A) **1**, separate granules; (B) **2**, cluster of threads; (C) **1**, threads; (D) **2**, small threads emanating from cluster of granules and threads. Bars indicate 100 nm. Pt-shadowing was used in all instances.

polymers **1** and **2**: these structures require a *directionality* in the assembly process.

3. Conclusion

TEM microscopy studies on surfaces onto which poly(ethylene oxide) amphiphiles **1**−**3** were deposited from aqueous solutions have revealed spherical (granular) and threadlike structures. Such structures are typically found for amphiphilic aggregates. However, in this case, the formation of the assemblies stems from amphiphiles with an unconventional design—i.e. amphiphiles with an unconventional primary structure. The formation of especially the threadlike structures can be regarded as surprising: for the formation of such higher structures, a directionality in the assembling process is necessary. A comparative ORD analysis on polymers **1**−**3** and on reference components has been performed to obtain indications for the origin of this directionality. Assuming that an inversion of optical rotation in the studied examples of chiral ethylene oxides stems from a transition from a random conformation to a helical conformation, it is proposed that polymer **3** and possibly polymers **1** and **2** adopt helical conformations in H_2O.

Summarized, ORD data indicate that polymers **1**−**3** form helically ordered secondary structures in H_2O, and TEM-pictures show the formation of higher structures that require a specific assembly process. However, there is no substantial evidence that the aggregation of **1**−**3** in H_2O is accompanied by the formation of the unique coiled-coil tertiary structure.

Experimental Section

General. Commercially available compounds employed in the syntheses were used without further purification, except stannous octanoate ($SnOct_2$), which was distilled *in vacuo* in a Kugelrohr apparatus (0.3 mbar, 200−220 °C) and stored in a glovebox. Solvents were dried and distilled if necessary, and reactions were routinely carried out under an inert atmosphere of dried argon or nitrogen. Details on the devices, materials, and methods are collected the Experimental Section (General) of Part 1.

ORD Experiments. ORD spectra were recorded on a JASCO DIP 370 spectropolarimeter. Depending on the applied concentrations, sample holders of 1 cm or 1 dm were used.

Additional Data on Figure 3. For plots A, B, C, and D polymers **1**, **2**, **3**, and again **3** were used, respectively. The polymer batches that were used correspond to entries **B**, **G**, **J**, and **I** from Table 1 in Part 1. Plot A: concentrations of 2.4, 1.8, 3.2 and 2.9 mg/mL were used in the solutions of THF, THF/H_2O, EtOAc, and MeOH. Plot B: concentrations of 11.1, 9.5, 10.2, and 9.3 mg/mL were used in the solutions of THF, THF/H_2O, MeOH, and MeOH/H_2O. Plot C: concentrations of 13, 13, 26, and 22 mg/mL were used in the solutions of EtOAc, THF, MeCN, and MeOH. Plot D: concentrations of 2.3, 2.2, 2.0, 1.7, 1.1, and 1.2 mg/mL were used in the THF/H_2O-solvent mixtures, containing 0%, 6%, 17%, 31%, 55%, and 100% (v/v) H_2O, respectively. A plot similar to plot D (not pictured in Figure 3) could also be produced by dissolving polymer **3** (entry **J** in Table 1 in Part 1) in THF/H_2O solvent mixtures at concentrations of 21.0, 15.9, 13.1, and 8.7 mg/mL and water contents of 0%, 18%, 32%, and 47% (v/v), respectively.

Additional Data on Figure 4. In plot A, *(SS)*-**4** was measured in aqueous solutions of MeOH containing 0%, 6%, and 21% H_2O (v/v). Concentrations of 4.8, 4.5, and 3.8 mg/mL were applied, respectively. Polymer **7** prepared by procedure B (*vide infra*) has been used for plot B. Concentrations of 3.2, 3.1, and 2.7 mg/mL were used for the dioxane, dioxane/H_2O, and EtOAc solutions.

Additional Data on Figure 5. Polymer **3** corresponding to entries **H** and **K** in Table 1 (see Part 1), respectively, has been used for plots A and B.

Additional Data on Figure 7. In plots A and C of Figure 7, a concentration of 0.34 mol/L *of (SS)*-**4** has been used. In plot B the cumulative concentration of glycol and salt was kept constant (a requirement for Job plots): [KSCN] + [*(SS)*-**4**] = 0.145 mol/L. In plot D a concentration of 0.0357 mol/L of *(SS)*-**4** was applied (employed temperature: 25 °C). The diquinolinyl glycol *(SS)*-**6** was titrated in CD_3OD with KSCN at a concentration of 0.013 mol/L. The carbon shifts of two carbons have been used to determine the *K* value. The titration of ether **5** with KSCN at a concentration of 0.30 mol/L was also monitored by ^{13}C NMR. In this case, only one carbon signal was selected to obtain the *K* value. Errors in the obtained *K* values for the 1:1 complexes of KSCN with *(SS)*-**4**, **5** and *(SS)*-**6** did not exceed 15%. Unless mentioned otherwise, the titrations were executed in MeOH or in CD_3OD at 20 °C.

Additional Information on Figure 8. For plot A, *(SS)*-**4** was dissolved in MeOH at a concentration of 8.3 mg/mL (=0.0145 mol/L) and was titrated with 0, 1.7, 4.0, 10.9, and 24.8 mol equiv of KSCN, respectively. For plot B, *(SS)*-**6** was dissolved in MeOH at a concentration of 13.05 mg/mL (=0.020 mol/L) and was titrated with 0, 0.48, 0.97, 1.8, 4.5, and 8.9 mol equiv of KSCN, respectively.

Complexation Experiments. Attempts To Obtain Solid Complexes of Glycols *(SS)*-4, 5, and *(SS)*-6 with KSCN or RbI (in the Case of *(SS)*-6). Both the ethylene oxide and the salt were dissolved in Me_2CO or MeOH/EtOAc solvent mixtures and maintained at reflux overnight. Neither addition of petroleum ether nor cooling to 4 °C resulted in the crystallization of a complex.

Microscopy Measurements. All grids were studied with a Philips TEM 201 (60 kV). TEM-samples were prepared by dissolving **1**, **2**, or **3** in a minimum amount of Me_2CO or MeCN and diluting the solutions with H_2O to the desired concentrations (the amount of Me_2CO or MeCN in the aqueous solutions always was <1%). Concentrations of the final solutions of **1**, **2**, and **3** varied from 2×10^{-4} to 8×10^{-3} mg/mL, from 5×10^{-5} to 0.3 mg/mL and from 2×10^{-3} to 5 mg/mL, respectively. Droplets of these solutions were brought on Cu grids covered with carbon or polymer (formvar) surfaces. The droplets were either removed after 1 min or allowed to evaporate overnight, thus varying the deposition time of the polymeric material on the substrates substantially. The best results were obtained when dilute solutions of the polymer were used (concentrations in the range 2×10^{-4} to 3×10^{-2} mg/mL) and when the droplets were allowed to evaporate overnight. Finally, mainly Pt-shadowing, and sometimes negative staining, was used to make detection of the formed structures possible. Negative staining was performed by placing a droplet of a 2 (w/w) uranyl acetate ($UO_2(OCOCH_3)_2$) aqueous solution onto the Cu grid and removing it after 15 s. Pt-shading was performed by placing the Cu grid in a Balzers sputter unit.

Granular (spherical) and threadlike structures were observed on most grids, and usually these structures were found in clusters. In one case, vesicle-like structures were found. The granular structures were found for polymers **1**, **2**, and **3**. The diameters of the granules were typically in the order of 50 nm. Clusters of the granules had no specific appearance but had diameters in the order of 800 nm. Threadlike structures were only found for the isobutyl-substituted polymers **1** and **2**. The clusters of the threadlike structures had diameters in the order of 1000 nm. The 'threads' varied in diameter from 8 to 50 nm and varied in length from 80 to 400 nm. Often, the clusters of the 'threads' also contained the previously mentioned granules. Finally, 'vesicles' were found for polymer **2**. Outer diameters and thicknesses of the 'bilayers' of ca. 150 and 50 nm were observed, respectively. (*Note:* None of the found structures were frequently spread over the surfaces of the grids.)

AFM samples were prepared by dissolving polymer **2** in MeCN and diluting the solution with H_2O to concentrations of 3×10^{-3} and 2.5×10^{-4} mg/mL. Droplets of these solutions were brought on a Si-wafer substrate and were allowed to evaporate. STM samples were prepared by dissolving polymer **1** and **2** in Me_2CO and diluting the solutions with H_2O to concentrations of 4×10^{-3} and 5×10^{-4} mg/mL. The droplets were brought on a crystalline Cu substrate, that had been etched electrochemically. The droplets were allowed to evaporate. The AFM/STM measurements were performed in an ultrahigh vacuum chamber (base pressure 10^{-10} mbar) with an Omicron apparatus. The AFM detection mechanism is based on the beam-deflection method. The normal and lateral forces experienced by the rectangular cantilever with the integrated silicon tip were calibrated.

1-((2-Methoxyethoxy)methoxy)-17-(benzyloxy)-3,6,9, 12,15-pentaoxaheptadecane (5). *O*-Benzyl hexaethylene glycol (0.48 g, 1.34 mmol) was coevaporated with PhMe and thereafter dissolved in 2 mL of distilled CH_2Cl_2 containing N(i-Pr)$_2$Et (330 mg, 2.56 mmol). The solution was cooled to 0 °C, MEMCl (380 mg, 3.05 mmol) was added dropwise, and the solution was stirred at reflux overnight. CH_2Cl_2/H_2O extraction—the pH of the water layer was kept at 2—drying of the collected organic layers and evaporation of the solvent gave 0.65 g of crude product. Silica column chromatography applying CH_2Cl_2/MeOH (20/1) as eluent and subsequent column chromatography using EtOAc/MeCN (4/1) as eluent gave a clear, yellowish oil. Yield: 400 mg (68%). ^1H NMR ($CDCl_3$): δ 7.3 (5H, m, Ph), 4.7 (2H, s, OCH_2O), 4.6 (2H, s, OCH_2Ph), 3.7−3.6 (26H, m), 3.55 (2H, m), 3.4 (3H, s). ^{13}C NMR ($CDCl_3$): δ 138.0, 128.1, 127.5, 127.3 (Ph), 73.0 (O*C*H$_2$Ph), 95.4 (O*C*H$_2$O), 58.8 (O*C*H$_3$), 71.5, 70.4, 70.3 (8×), 70.2, 69.2, 66.6, 66.5. ^1H NMR (CD_3OD): δ 7.3 (5H, m, Ph), 4.7 (2H, s, OCH_2O), 4.55 (2H, s, OCH_2Ph), 3.7−3.6 (26H, m), 3.5 (2H, m), 3.3 (3H, s). ^{13}C NMR (CD_3OD): δ 139.7, 129.3, 128.8, 128.6 (Ph), 96.5 (O-*C*H$_2$-O), 59.1 (O*C*H$_3$), 74.0, 72.9, 71.5 (9×), 71.4, 70.6, 68.0, 67.8. FTIR (cm^{-1}): ν = 2868, 1454, 1351, 1296, 1248, 1115, 946, 851, 741, 700.

(4*S*,13*S*)-1,17-(Di-8-quinolinoxy)-4,13-diisobutyl-3,6,9, 12,15-pentaoxaheptadecane ((*SS*)-6). A solution of α,ω-ditosylate *(SS)*-**9** (170 mg, 0.24 mmol) in 2.5 mL of THF and 0.5 mL of HMPA (hexamethylphosphoramide) was added to a boiling suspension of 8-hydroxyquinoline (81.5 mg, 0.56 mmol) and KOH (85%, 36 mg, 0.55 mmol) in 0.5 mL of THF and 0.5 mL of HMPA. The suspension, which turned green and became turbid, was kept at reflux overnight. Thereafter, H_2O and KOH were added to the reaction mixture and the aqueous solution was extracted with CH_2Cl_2. The collected organic layers were dried with Na_2SO_4, and evaporation of the solvent gave a crude oily product. Sequential elution on an alumina column with hexane/EtOAc (1/1) and with EtOAc gave 130 mg of product (85%). Clear oil. ^1H NMR ($CDCl_3$): δ 8.9 (2H, m), 8.1 (m, 2H), 7.4 (m, 6H), 7.1 (m, 2H), 4.4 (4H, m), 4.2 (1H, ddd, ^2J = 10.9 Hz, ^3J = 5.9 Hz, ^3J = 5.9 Hz), 4.1 (3H, m), 3.75 (1H, m), 3.6−3.5 (13H, m), 1.70 (2H, m), 1.45 (2H, m), 1.25 (2H, m), 0.90 (12H, × 4 d, ^3J = 7.0 Hz (2×) and 6.6 Hz (2×)). ^{13}C NMR ($CDCl_3$): δ 154.6, 154.5, 149.1, 149.0, 140.3 (2'),

135.7, 135.6, 129.3 (2×), 126.5 (2×), 121.4, 121.3, 119.7, 119.6, 109.2, 109.1 (quinoline carbons), 41.0, 40.9, 24.3, 24.2, 23.2 (2 ×), 22.1 (2×) (isobutyl carbons), 77.8, 77.3, 74.5, 74.3, 70.7, 70.6, 70.4, 69.5, 69.2, 68.1, 68.0, 67.8. ^{1}H NMR (CD_3OD): δ 8.8 (2H, m), 8.3 (m, 2H), 7.5 (m, 6H), 7.2 (m, 2H), 4.35 (4H, m), 4.2−3.9 (4H, m), 3.7 (1H, m), 3.6 (1H, m), 3.6−3.4 (12H, m), 1.70 (2H, m), 1.35 (2H, m), 1.2 (2H, m), 0.80 (12H, 4 × d, ^3J = 6.7 Hz (2×), 6.6 and 6.2 Hz). ^{13}C NMR (CD_3OD): δ 149.8 (2'), 147.0 (2×), 140.6 (2×), 138.0 (2×), 130.1 (2×), 128.3 (2×), 122.9 (2×), 120.9, 120.8, 110.8, 110.7 (quinoline carbons), 42.3 (2×), 25.6 (2×), 23.8 (2×), 22.7 (2×) (isobutyl carbons), 79.0, 78.7, 75.4, 75.2, 71.9, 71.8, 71.5, 70.8, 70.4, 69.7, 69.6, 69.4. $[\alpha]^{25}_D = -12.3°$ (c = 4.60; THF). $[\alpha]^{25}_D = -11.7°$ (c = 3.25; THF). TLC: R_f (hexane/EtOAc (1/1) silica) = 0.25; R_f (EtOAc, silica) = 0.80; R_f (hexane/EtOAc (1/1), alumina) = 0.05; R_f (EtOAc, alumina) = 0.38. HRMS: Calcd, 648.3775; found, 648.3803. UV maxima in MeOH were recorded at 305 and 240 nm (ϵ = 8.5 and 96.3 L × g^{-1} × cm^{-1}, respectively). These maxima shifted to 252 and 358 nm after protonation of the pyridine moiety with HCl.

Poly(4*(S)*-methyl-ϵ-caprolactone) (7). This polymer was obtained by polymerization of (4*S*)-4-methyl-ϵ-caprolactone. Purification of the monomer was achieved by silica column chromatography using CH_2Cl_2/EtCOMe (8/1) as eluent (R_f = 0.50).[28] The (enantiomeric) purity of the lactone was checked on a β-cyclodextrin GC column, that was processed at 145 °C: no traces of contaminants were found. ^{1}H NMR ($CDCl_3$): δ 4.2 (1H, m), 4.1 (1H, m), 2.65 (2H, m), 1.90 (2H, m), 1.75 (1H, m), 1.45 (1H, m), 1.30 (1H, m), 0.95 (3H, d). ^{13}C NMR ($CDCl_3$): δ 176.0 (CO), 22.0 (CH_3), 68.0 (OCH_2), 37.1, 35.1, 33.1, 30.7. $[\alpha]^{20}_D = -53.8$ ° (c = 0.77; CH_2Cl_2). FTIR (cm^{-1}): ν = 2957, 2927, 2872, 1740, 1478, 1448, 1389, 1339, 1306, 1282, 1255, 1163, 1095, 1079, 1008, 935, 862, 796, 730, 711, 585, 522. GC-MS (FW = 128): 128 and 129 (with abundances of 4.2% and 0.5%, respectively).

Procedure A. (4*S*)-4-Methyl-ϵ-caprolactone (104 mg, 0.81 mmol) and 10 μL of a 0.10 M solution of $SnOct_2$ in PhMe (monomer/catalyst ratio of 810/1) were mixed under an argon atmosphere at 140 °C in a silylated Schlenk flask. After 24 h the oily product was dissolved in $CHCl_3$ and precipitated in MeOH. The polymer was collected as a sticky yellowish oil. Yield: 36 mg (35%). SEC: M_n = 29.7 kg/mol, D = 1.36 (data obtained with PS standards).

Procedure B. (4*S*)-4-Methyl-ϵ-caprolactone (56 mg, 0.44 mmol) and 9 μL of a 0.50 M solution of $SnOct_2$ in PhMe (monomer/catalyst ratio of 98/1) were mixed under an argon atmosphere at 110 °C in a silylated Schlenk flask for 3 h. Further reaction at 140 °C for 24 h gave an oily product that was dissolved in CH_2Cl_2 and precipitated in hexane/ether (4/1). The polymer was collected as a sticky yellowish oil. Yield: 32 mg (57%). SEC: M_n = 8.4 kg/mol, D = 2.3 (data obtained with PS standards). This polymer was used for the ORD measurements in Figure 4. ^{1}H NMR ($CDCl_3$): δ 4.15 (2H, m), 2.30 (2H, m), 1.8−1.4 (5H, m), 0.95 (3H, d, ^3J = 6.6. Hz). ^{13}C NMR ($CDCl_3$): δ 173.7, (CO), 19.0 (CH_3), 62.6 (OCH_2), 35.2, 31.9, 31.7, 29.5.

(4*S*,13*S*)-1,17-Bis(tosyloxy)-4,13-diisobutyl-3,6,9,12,15-pentaoxaheptadecane ((*SS*)-9). (4*S*,13*S*)-4,13-Diisobutyl-17-hydroxy-3,6,9,12,15-pentaoxaheptadecanol (110 mg, 0.28 mmol, *(SS)*-**8**) and tosyl chloride (118 mg, 0.62 mmol) were dissolved in 0.4 mL of distilled CH_2Cl_2. The solution was cooled in an ice bath. Finely ground KOH (85%, 130 mg, 1.97 mmol) was added in four portions over a 15-min period, after which the suspension was stirred for 3 h. Ice water and CH_2Cl_2 were added to the reaction mixture, and extraction of the H_2O layer was executed. Drying of the organic layers with $MgSO_4$ and evacuation of the solvent yielded 210 mg of crude product. Sequential elution on a silica column with hexane/EtOAc (3/1)—to remove the TsCl contaminant—and with EtOAc gave an oily product. Yield: 170 mg (87%). ^{1}H NMR (CD_3CN): δ 7.8 (4H, m), 7.4 (4H, m), 4.1 (6H, m), 3.8 (1H, ddd, ^2J = 12.2 Hz, ^3J = 4.8 Hz, ^3J = 4.1 Hz), 3.6 (3H, m), 3.4 (12H, m), 2.45 (s, 6H), 1.65 (2H, m), 1.30 (2H, m), 1.20 (2H, m), 0.85 (12H, 4 × d, ^3J = 6.6 Hz (2×), 6.3 and 6.2 Hz). ^{13}C NMR (CD_3CN): δ 146.3, 146.2, 133.9 (2×), 131.0 (2×), 128.8(2×) (Ts), 41.8, 41.7, 25.2, 25.1, 23.6 (2×), 22.7, 22.5 (isobutyl carbons), 21.7, 21.1 ($PhCH_3$), 78.2, 77.9, 74.9, 74.5, 71.6, 71.5, 71.4, 71.1, 70.9, 69.9, 69.3, 68.2. $[\alpha]^{25}_D = -12.3°$ (c = 4.60; THF). TLC: R_f (hexane/EtOAc (1/1), silica) = 0.25; R_f (EtOAc, silica) = 0.80.

Acknowledgment. *(S)*-4-Methyl-ϵ-caprolactone was kindly provided by Margaret Kayser and Gang Chen (University of New Brunswick, Saint John, Canada).[23] Peter Buijnsters, Huub Geurts (University of Nijmegen), and Wieb Kingma are acknowledged for the TEM data and the SEC measurements.

References and Notes

(1) This is the second part of a back-to-back article sequence. Additionally, a previous communication has reported on the first results on this research topic: Janssen, H. M.; Peeters, E.; van Zundert, M. F.; van Genderen, M. H. P.; Meijer, E. W. *Angew. Chem.* **1997**, *109*, 152 (*Angew. Chem., Int. Ed. Engl.* **1997**, *36*, 122).

(2) Mann, S. *Biomimetic materials chemistry*; VCH Publishers Inc.: New York, 1996.

(3) Percec, V.; Heck, J. A.; Lee, M.; Ungar, G.; Alvarez-Castillo, A. *J. Mater. Chem.* **1992**, *2*, 1033. Percec, V.; Johansson, G.; Heck, J. A.; Ungar, G.; Batty, S. V. *J. Chem. Soc., Perkin Trans. 1* **1993**, 1411. Percec, V.; Heck, J. A.; Tomazos, D.; Ungar, G. *J. Chem. Soc., Perkin Trans. 2* **1993**, 2381. Percec, V.; Heck, J. A.; Tomazos, D.; Falkenberg, F.; Blackwell, H.; Ungar, G. *J. Chem. Soc., Perkin Trans. 1* **1993**, 2799.

(4) Peptides such as α-keratin, myosin, and tropomyosin (the latter two are muscle proteins) exhibit coiled-coil superstructures. Stryer, L. *Biochemistry*, 4th ed.; W. H. Freeman & Company: New York, 1995.

(5) Crick, F. H. C. *Nature* **1952**, *170*, 882. Crick, F. H. C. *Acta Crystallogr.* **1953**, *6*, 689.

(6) O'Shea, E. K.; Klemm, J. D.; Kim, P. S.; Alber, T. *Science* **1991**, *254*, 539.

(7) Landschulz, W. H.; Johnson, P. F.; McKnight, S. L. *Science* **1988**, *240*, 1759. O'Shea, E. K.; Rutkowski, R.; Kim, P. S. *Science* **1989**, *243*, 538. Harbury, P. B.; Zhang, T.; Kim, P. S.; Alber, T. *Science* **1993**, *262*, 1401. Gronenborn, A. M.; Clore, G. M. *Science* **1994**, *263*, 536. Cohen, C.; Parry, D. A. D. *Science* **1994**, *263*, 488. Kazmierski, W. M.; McDermed, J.; Aulabaugh, A. *Chem. Eur. J.* **1996**, *2*, 403.

(8) Hodges, R. S.; Sodek, J.; Smillie, L. B.; Jurasek, L. *Cold Spring Harbor Symp. Quant. Biol.* **1972**, *37*, 299. O'Shea, E. K.; Rutkowski, R.; Statford, W. F., III; Kim, P. S. *Science* **1989**, *245*, 646. Junius, F. K.; Weiss, A. S.; King, G. F. *Eur. J. Biochem.* **1993**, *214*, 415. Malashkevich, V. N.; Kammener, R. A.; Efimimov, V. P.; Schulthess, T.; Jürgen, E. *Science* **1996**, *274*, 761.

(9) O'Neill, K. T.; Hoess, R. H.; DeGrado, W. F. *Science* **1990**, *249*, 774. Zhou, N. E.; Kay, C. M.; Hodges, R. S. *Biochemistry* **1992**, *31*, 5739. Graddis, T. J.; Myszka, D. G.; Chaiken, I. M. *Biochemistry* **1993**, *32*, 12644. Houston, M. E.; Campbell, A. P.; Lix, B.; Kay, C. M.; Sykes, B. D.; Hodges, R. S. *Biochemistry* **1996**, *35*, 10041.

(10) Vogl, O.; Jaycox, G. D.; *Polymer* **1987**, *28*, 2179.

(11) Murdoch, J. R.; Loomis, G. L. U.S. Patent 4,719,246. Ikada, Y.; Tsuji, H. *Macromolecules* **1993**, *26*, 6918 and references therein. Nubuhiku, Y.; Dijkstra, P. J.; Feijen, J. *Makromol. Chem.* **1990**, *191*, 481.

(12) Watanabe, W. H.; Ryan, C. F.; Fleischer, P. C.; Garrett, B. S. *J. Phys. Chem.* **1961**, *65*, 896. Liquori, A. M.; Anzuino, G.; d'Alagni, M.; Coiro, V. M.; de Santis, P.; Savino, M. *Nature* **1965**, *206*, 358. Schomaker, E. The process of stereocomplexation between it-PMMA and st-PMMA. Thesis from the University of Groningen, 1988.

(13) Recently, information has been published about synthetic phenylacetylene oligomers that fold into helical arrangements as a result of hydrophobic effects: Nelson, J. C.; Saven, J. G.; Moore, J. S.; Wolynes, P. G. *Science* **1997**, *277*, 1793.

(14) Takahashi, Y.; Tadokoro, H. *Macromolecules* **1973**, *6*, 672.

(15) Matsuura, H.; Fukuhara, K. *J. Mol. Struct.* **1985**, *126*, 251.

(16) For example in: Zhou, N. E.; Kay, C. M.; Hodges, R. S. *Biochemistry* **1992**, *31*, 5739.

(17) Volkenstein, M. V. *Configurational statistics of polymer chains*, Interscience: New York, 1963; p 139.

(18) *Encyclopedia of polymer science and engineering: Helix-coil transitions*, 2nd ed.; Mark, H. F., Bikales, N. M., Overberger, C. G., Menges, G., Eds.; John Wiley & Sons: New York, 1987; Vol. 7, pp 685−698. Blout, E. R. In *Optical rotatory dispersion and circular dichroism in organic chemistry*; Snatzke, G., Ed.; Heyden and Son: London, 1967.

(19) For poly(γ-benzyl-L-glutamate) and poly(β-benzyl-L-aspartate), clear-cut changes in specific rotation have been observed at 68% and 8% dichloroacetic acid in $CHCl_3$, respectively, indicating coil-to-helix transitions. Karlson, R. H.; Norland, N. S.; Fasman, G. D.; Blout, E. R. *J. Am. Chem. Soc.* **1960**, *82*, 2268. Doty, P.; Wada, A.; Yang, J. T.; Blout, E. R. *J. Polym. Sci.* **1957**, *23*, 851.

(20) Pino, P. In *Optical rotatory dispersion and circular dichroism in organic chemistry*; Snatzke, G., Ed.; Heyden and Son: London, 1967. Chiellini, E.; Salvadori, P.; Osgan, M.; Pino, P. *J. Polym. Sci. A-1* **1970**, *8*, 1589. Pino, P.; Salvadori, P.; Chiellini, E.; Luisi, P. L. *Pure Appl. Chem.* **1968**, *16*, 469.

(21) Tsunetsugu, T.; Furukawa, J.; Fueno, T. *J. Polym. Sci. A-1* **1971**, *9*, 3529 and 3541. Hirano, T.; Sato, A.; Tsuruta, T.; Johnson, W. C. *J. Polym. Sci., Polym. Phys. Ed.* **1979**, *17*, 1601.

(22) Peeters, E.; Janssen, H. M.; van Zundert, M. F.; van Genderen, M. H. P.; Meijer, E. W. *Acta Polym.* **1996**, *47*, 485.

(23) *(S)*-4-Methyl-ϵ-caprolactone and similar compounds with ee values exceeding 99% have been described in: Stewart, J. D.; Reed, K. W.; Kayser, M. M. *J. Chem. Soc. Perkin Trans. 1* **1996**, 755. Stewart, J. D.; Reed, K. W.; Zhu, J.; Chen, G.; Kayser, M. M. *J. Org. Chem.* **1996**, *61*, 7653.

(24) See Part 1 of this article sequence.

(25) Steinberg, I. Z.; Harrington, W. F.; Berger, A.; Sela, M.; Katchalski, E. *J. Am. Chem. Soc.* **1960**, *82*, 5263. Blout, E. R.; Carver, J. P.; Gross, J. *J. Am. Chem. Soc.* **1963**, *85*, 644. Gratzer, W. B.; Rhodes, W.; Fasman, D. G. *Biopolymers* **1963**, *1*, 319. Pohl, F. M.; Jovan, T. M. *J. Mol. Biol.* **1972**, *67*, 375. Letsinger, R. L. *Proc. Robert A. Welch Found. Conf. Chem. Res.* **1985**, *29*, 459. Cosstick, R.; Eckstein, F. *Biochemistry* **1985**, *24*, 3630. McIntosh, L. P.; Zielinski, W. S.; Kalish, B. W.; Pfiefer, G. P.; Sprinzl, M.; van der Sande, J. H.; Jovin, T. M. *Biochemistry* **1985**, *24*, 4806. Pu, Y. M.; McDonagh, A. F.; Lightner, D. A. *J. Am. Chem. Soc.* **1993**, *115*, 377.

(26) Vögtle, F.; Weber, E. *Angew. Chem., Int. Ed. Engl.* **1979**, *18*, 753. Weber, E.; Vögtle, F. *Tetrahedron Lett.* **1975**, 2415. Tümmler, B.; Maass, G.; Weber, E.; Wehner, W.; Vögtle, F. *J. Am. Chem. Soc.* **1977**, *99*, 4683. Tümmler, B.; Maass, G.; Vögtle, F.; Sieger, H.; Heimann, U.; Weber, E. *J. Am. Chem. Soc.* **1979**, *101*, 2588. Vögtle, F.; Sieger, H. *Angew. Chem., Int. Ed. Engl.* **1977**, *16*, 396. Vögtle, F.; Sieger, H. *Angew. Chem.* **1978**, *90*, 212. Sieger, H.; Vögtle, F. *Tetrahedron Lett.* **1978**, 2709.

(27) Preliminary and brief AFM studies on polymer **2** as well as STM studies on polymers **1** and **2** did not reveal any well-defined structures. The size of peptide based coiled coils is in the order of 2 nm in diameter, 14 nm in pitch, and 150 nm in length, and therefore, these and other tertiary structures can in principle most ideally be studied by AFM or STM.

(28) An aqueous 5% KI/I_2 solution was used as fixation liquid for the TLC plates.

(29) Saenger, W.; Brand, H.; Vögtle, F.; Weber, E. In *Metal−ligand interactions in organic chemistry and biochemistry;* Pullman, B., Goldblum, N., Eds.; Reidel: Dordrecht, 1977; p 363.

MA970939D